# Physics-Guided Data-Driven Failure Identification of Underwater Mooring Systems in Offshore Infrastructures

Yixuan Liu<sup>a</sup>, Shangyan Zou<sup>b</sup>, Qingbin Gao<sup>c</sup>, and Kai Zhou<sup>\*a</sup>

<sup>a</sup> The Hong Kong Polytechnic University, Hong Kong, China <sup>b</sup>Michigan Technological University, MI, USA <sup>c</sup>Harbin Institute of Technology, Shenzhen, China <sup>\*</sup>cee-kai.zhou@polyu.edu.hk

## ABSTRACT

Many offshore infrastructures have been developed to explore vast marine resources over the past several decades. In addition to the conventional fixed-type offshore infrastructures, a new class of offshore infrastructures, the so-called floating offshore infrastructures, have gained dramatically increasing applications owing to their flexible deployment and enhanced capacity in renewable energy exploitation in deep seawater. As the key functional component of the floating infrastructure, the underwater mooring systems are subject to sustained dynamic loads pertinent to marine waves and currents, which are prone to different types of failures. Identifying those mooring system failures timely and reliably thus plays a vital role in offshore infrastructure health management and maintenance. This study aims to achieve this objective by developing an integrated numerical framework that seamlessly synthesizes the physical mooring system modeling and data-driven analysis. Specifically, a high-fidelity physical model that takes into account the sophisticated fluid-structure interaction is established to mimic the underlying behavior of the mooring system. The mooring line failures are incorporated into the model to generate the respective dynamic responses. With the aid of data-driven modeling, the causative relationship between mooring line failure scenarios and dynamic responses can be characterized. Given the sensor measurement in actual practice, this framework offers a feasible solution for the failure identification of underwater mooring systems. The results clearly demonstrate the feasibility of the proposed methodology.

**Keywords:** Offshore infrastructure, underwater mooring systems, integrated numerical framework, physical mooring system modeling, failure identification.

#### 1. INTRODUCTION

As the global demand for green and clean energy grows, offshore energy infrastructures, especially floating structures, have been rapidly developed in areas such as wind energy utilization and offshore oil and gas development in deep water areas. The floating platform relies on a mooring system to connect to the seabed, and its stability depends on the integrity and reliability of the mooring system. However, the inherent complexity and harshness of the marine environment pose continuous physical and chemical erosion challenges to the mooring system, increasing its probability of failure. The failure of the mooring system can cause entire platform failures, leading to energy production losses, costly repairs, and potential environmental disasters.<sup>1,2</sup> Therefore, effective monitoring technology, aiming at ensuring the safety of mooring systems is essential.

The traditional monitoring of mooring systems primarily relies on visual inspections conducted by divers or underwater drones.<sup>3</sup> While the method is straightforward and effective, it is heavily dependent on weather conditions and ocean depths and is less feasible for internal or micro-level damages. Actual inspection data for offshore floating structures is scarce and expensive. Researchers are looking for methods based on physical models to predict failures, but constantly updating numerical models will bring huge computational costs.<sup>4–6</sup> Considering the reliability of the physical model and the flexibility of the data-driven model, a damage detection method is proposed that leverages the strengths of both. This method utilizes the prior knowledge provided by physical models and the strong learning capabilities of data-driven models to efficiently monitor and accurately identify damages in mooring systems.

In the field of mooring system monitoring, changes in stiffness parameters are considered to be key indicators reflecting structural integrity, which have a significant impact on the dynamic response of the floating platform, thereby affecting the internal tension and overall stability of the mooring line.<sup>7,8</sup> The application of signal processing techniques for structural damage detection has been validated through research.<sup>9,10</sup> Furthermore, machine learning algorithms, especially neural networks, show broad application potential in the field of damage detection based on signal processing. As one of the most popular and mature deep learning algorithms at present, convolutional neural networks (CNNs) are the primary architectures for various neural network variants.<sup>11</sup> It has achieved remarkable success in many fields such as image recognition and natural language processing.<sup>12,13</sup> Due to its powerful capabilities in feature extraction and pattern recognition, more and more scholars are paying attention to the effectiveness of CNN models in the fields of structural monitoring and damage detection.<sup>14,15</sup> This study focuses on exploring the application of physics-guided data-driven methods in the identification of faults in offshore mooring systems. Specifically, by integrating a fluid-structure interaction (FSI) physical model that accounts for changes in mooring line stiffness with a data-driven predictive analysis based on CNNs, this study aims to develop an efficient and effective method that can accurately identify and evaluate potential faults in mooring systems.

The rest of the article is organized as follows: Section 2 introduces the theoretical basis of fluid-structure interaction (FSI) physical modeling and the underlying principle behind the one-dimensional CNN model. Section 3 presents the construction process of the integrated framework, including the development of physical models, dataset generation, CNN architecture selection, and emulation, followed by the result presentation and discussion for framework validation. Section 4 concludes this work and outlines the future plan.

## 2. METHODOLOGY

In this section, we integrate fluid-structure interaction (FSI) physical modeling with data-driven approaches to accurately simulate and identify the dynamic behavior and potential structural damage in the mooring system of a floating structure. The core content consists of two key components: the establishment of an FSI physical model and the application of a one-dimensional CNN. This integrated framework will be practiced on the identification of mooring line stiffness reduction to demonstrate its effectiveness.

## 2.1 Principle for fluid-structure interaction (FSI) physical modeling

In order to replicate the dynamic behavior of floating offshore structures in the marine environment, a fluid-structure interaction modeling approach will be adopted in this study. First of all, the three-dimensional potential flow theory was employed to determine the fluid dynamic loads. This theory decomposes the flow field velocity potential into three parts,

$$\Phi(x, y, z, t) = \Phi_r + \Phi_\omega + \Phi_d, \tag{1}$$

where x, y, and z are the position coordinates of the floating structure along three directions respectively. t is the time variable.  $\Phi_r$  is the radiation potential, which is generated by changes in the flow field caused by the movement of the floating structure.  $\Phi_{\omega}$  is the incident potential of the wave that is not interfered with by the floating structure.  $\Phi_d$  represents the wave diffraction potential generated after the wave passes through the floating structure. The boundary conditions that each velocity potential needs to satisfy are as follows:  $^{16}$  Laplace's Equation:

$$\frac{\partial^2 \Phi}{\partial x^2} + \frac{\partial^2 \Phi}{\partial y^2} + \frac{\partial^2 \Phi}{\partial z^2} = 0, \qquad (2)$$

Seabed Boundary Condition:

$$\frac{\partial \Phi}{\partial z} = 0, z = -d, \tag{3}$$

Free Surface Condition:

$$\frac{\partial^2 \Phi}{\partial t^2} + g \frac{\partial \Phi}{\partial z} = 0, z = 0. \tag{4}$$

The mooring system uses catenary mooring cables, which connect the seabed through suspended steel anchor chains. The geometric effect of the catenary cables and the anchor chain's gravity generates a restoring force to

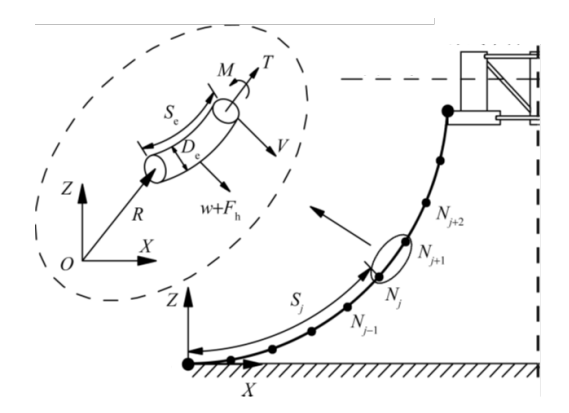


Figure 1. Modeling of a dynamic mooring line and the forces on a mooring element.

achieve the positioning of the floating platform. The mooring line is composed of N Morrison units of uniform size, with identical density and dimensional characteristics for each segment, <sup>17</sup> as shown in Fig. 1. The motion equation of the single unit of the mooring line in Fig. 1 can be simplified to

$$\frac{\partial \mathbf{T}}{\partial S_e} + \frac{\partial \mathbf{V}}{\partial S_e} + \mathbf{w} + \mathbf{F}_h = m_e \frac{\partial^2 \mathbf{R}}{\partial t^2}, \qquad (5)$$

$$\frac{\partial \mathbf{M}}{\partial S_e} + \frac{\partial \mathbf{R}}{\partial S_e} \mathbf{V} = -\mathbf{q} \,, \tag{6}$$

where T is the tension vector at the node of the mooring cable element. V is the shear force vector. R is the position vector. M is the bending moment vector.  $S_e$  is the unstretched length of the mooring cable element. w is the weight per unit length.  $F_h$  is the hydrodynamic load vector per unit length.  $m_e$  is the mass per unit length. q is the distributed moment load per unit length. Since the semi-submersible floating platform is represented as a six-degree-of-freedom (6-DOF) rigid body, the motion of this platform is governed by time-domain control equations,  $r_{ij}^{17,18}$  mathematically expressed as follows,

$$(\boldsymbol{M} + \boldsymbol{m}_{\infty}) \ddot{\boldsymbol{x}}(t) + \boldsymbol{D}\dot{\boldsymbol{x}}(t) + (\boldsymbol{K} + \boldsymbol{E})\boldsymbol{x}(t) + \int_{0}^{t} \boldsymbol{h}(t - \tau)\dot{\boldsymbol{x}}(\tau)d\tau = \boldsymbol{q}(t, \boldsymbol{x}, \dot{\boldsymbol{x}}),$$
(7)

where M and  $m_{\infty}$  are the structural and the fluid-added mass matrices at infinite frequency, respectively. D is the radiation damping matrix. K and E are the restoring matrix provided by static water and the mooring system. x(t),  $\dot{x}(t)$  and  $\ddot{x}(t)$  denote the displacement, velocity, and acceleration vectors of the platform, respectively. h(t) donates the acceleration impulse function matrix. q(t) q(t) is the excitation force vector, which includes wind loads, water flow loads, first and second-order wave loads, and the restoring forces provided by the mooring system.

# 2.2 One-dimensional (1D) convolutional neural network (CNN)

The study applies a one-dimensional CNN model for failure identification, the architecture of which typically consists of convolutional layers for feature extraction, pooling layers for downsampling and preserving the main features, and fully connected layers to map pivot features to damage prediction results. It is worth noting that the convolution and pooling operations in this study are performed along a single dimension, consistent with the characteristics of one-dimensional convolution.<sup>20,21</sup> This model is designed to automatically extract key features from time series data and enable effective damage identification.

The purpose of a convolutional layer is to extract features from the input data, which is implemented through filters (also known as convolution kernels or weights). For a one-dimensional convolution layer, its operation can be expressed as a convolution operation between the one-dimensional signal and the convolution kernel. For the convolution operation of the l layer, its output  $x_i^{(l+1)}$  can be expressed as

$$x_i^{(l+1)} = f\left(\sum_{j=1}^{M^{(l)}} conv1D\left(w_{ij}^{(l)}, x_j^{(l)}\right) + b_i^{(l)}\right), \tag{8}$$

where  $w_{ij}^{(l)}$  is the convolution kernel from the j-th feature map of layer l to the i-th feature map of layer l+1.  $b_i^{(l)}$  is the bias term. f is the activation function, such as ReLU, defined as f(x) = max(0, x). conv1D(...) donates the convolution operation between the convolution kernel and the feature map.

The pooling layer usually follows the convolutional layer, which tends to reduce the dimensionality of features while retaining the most important information. In one-dimensional pooling, the most commonly used operation is Max Pooling, which can be expressed as:

$$y_i^{(l+1)} = \max\left(x_i^{(l)}, x_{i+1}^{(l)}, \dots, x_{i+K-1}^{(l)}\right), \tag{9}$$

where K is the size of the pooling window. The Max pooling operation selects the maximum value in the window as the output value.

Finally, a fully connected (dense) layer is required, whose purpose is to map the extracted features to the target output, such as classification labels for a classification problem. The output of dense layer l can be calculated by the following formula,

$$z^{(l+1)} = f\left(W^{(l)}y^{(l)} + b^{(l)}\right), \tag{10}$$

where  $(W^{(l)})$  is the weight matrix.  $y^{(l)}$  is the output from the previous layer.  $b^{(l)}$  is the bias vector. f donates the activation function. Typically, in the fully connected layer, the Softmax function is used for multi-class classification. However, for regression tasks, the Softmax function is not used since regression aims to predict continuous values rather than class probabilities. Instead, other activation functions, such as identity functions (linear activation), are often applied to enable the network to provide continuous predictions. Although the general CNNs incorporates the three types of layers mentioned above, these layers can be combined in various ways to create different CNN architectures tailored to address specific problems, illustrating the high flexibility of CNN modeling.

#### 3. CASE ILLUSTRATION

In this section, we integrate the proposed methods to establish a comprehensive framework for effective damage identification in mooring systems. Given that this study primarily serves as a proof of concept, we will employ numerical experiments instead of actual experiments for data measurement, facilitating the damage identification process. The flow of this framework is illustrated in Fig. 2.

## 3.1 Physical model construction and data preparation

Given the absence of experimental data for model calibration, our approach involves constructing a high-fidelity physical model capable of accurately characterizing the actual system behavior. This section encompasses physical model construction, model refinement, selection through convergence analysis, and data generation for subsequent data-driven emulation analysis.

# 3.1.1 Platform FE model

Following Section 2.1, a benchmark model based on the actual OC4 semi-submersible floating platform in the South China Sea<sup>22,23</sup> is modeled by ANSYS AQWA<sup>16</sup> to simulate the numerical responses of the platform. The mooring system under the platform is comprised of three mooring lines to connect the platform with the seabed. The parameters of the entire model are based on the data published by the U.S. National Renewable Energy Laboratory (NREL),<sup>24</sup> which are summarized in Table 1. The corresponding finite element (FE) model with the load information is given in Fig. 3.

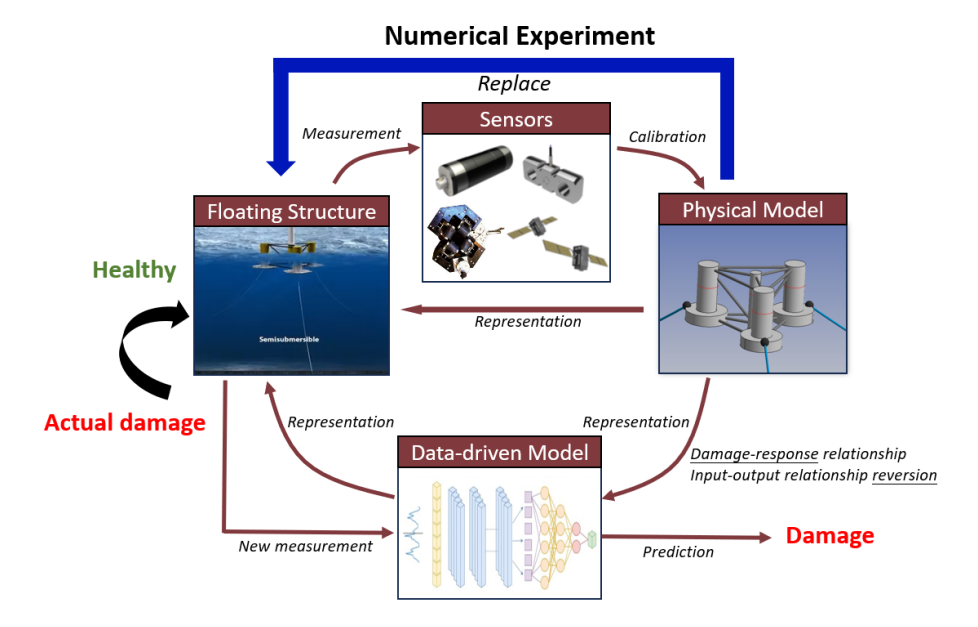


Figure 2. Implementation flowchart of the proposed framework.

Table 1. Platform parameters for FE modeling

Unstretched Line Length	835.5 m
Mooring Line Diameter	0.0766  m
Mooring Line Mass Density	113.35  kg/m
Mooring Line Stiffness	753.6MN
Platform Mass	$1.3473 E7 \ kg$
CM Location Below SWL	13.46 m
Platform Roll Inertia (CM)	6.827E9 kg · m <sup>2</sup>
Platform Pitch Inertia (CM)	$6.827 \mathrm{E}9~\mathrm{kg}\cdot\mathrm{m}^2$
Platform Yaw Inertia (CM)	$1.226\text{E}10~\text{kg}\cdot\text{m}^2$

To ensure accurate dynamic response measurements and capture the impact of damage, the model requires further validation. We conduct convergence analysis based on the finite element (FE) model, examining its accuracy with respect to mesh grid size and time increment. Several mesh size and time increment values are selected for analysis. The convergence degree is assessed by the relative error between the dynamic responses of two adjacent parameter values. Additionally, the computational cost of the model corresponding to different parameter values is also examined to inform suitable model selection. As an example, the convergence analysis results for the tension response of mooring line 2 are depicted in Fig. 4. Notably, the convergence trend observed in Fig. 4 aligns with those calculated for different dynamic responses and mooring lines. Considering the trade-off between the accuracy and computational cost, 1m mesh size and 0.05s time increment are chosen to establish the FE model for subsequent data generation.

#### 3.1.2 FE model-based data generation

To facilitate data-driven damage prediction, the damage information is incorporated into the FE model established in Section 3.1.1 to acquire damage-response relationships. Specifically, the stiffness reductions of mooring lines are considered to represent mooring system damage. Different combinations of mooring line stiffness reductions lead to the different dynamic responses of the floating platform. In this platform model, 9 different types of dynamic responses (i.e., the platform's responses (surge, sway, roll, pitch, heave, yaw) on 6 DOFs and tension changes of 3 mooring lines) are acquired, and their variations under different stiffness reduction combinations are demonstrated in Fig. 5.

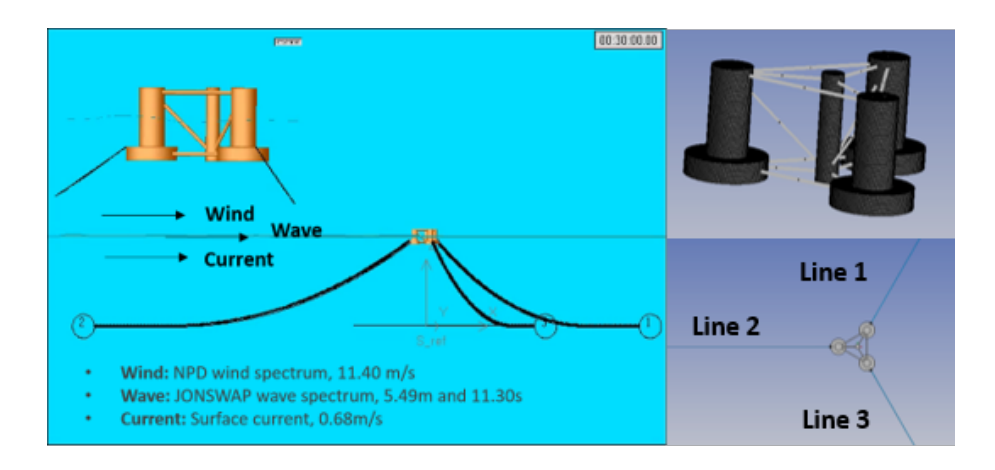


Figure 3. Illustration of FE model for the semi-submersible platform and its mooring system.

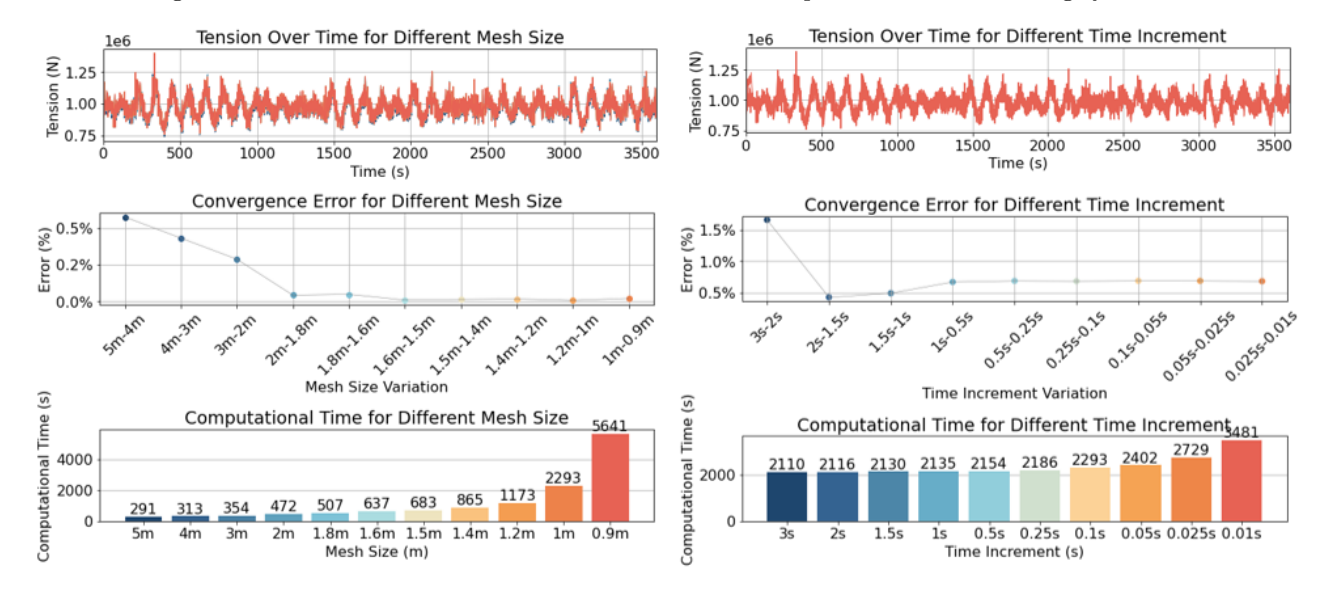


Figure 4. Convergence trend of tension response in mooring line 2 with different mesh sizes and time increments.

10 stiffness reduction coefficients are uniformly sampled (with a 10% increment) for each mooring line. Following such design of experiment (DOE), a total of 1,000 stiffness reduction samples for 3 mooring lines are generated to cover the entire parameter space. To streamline the whole analysis, an automated script was crafted using Python, executing from the sample generation, model updating, and analysis to dynamic response extraction. The above 1,000 stiffness reduction samples along with their respective dynamic responses form a database, which can be used for training subsequent machine learning models. Because of the unpredictable and stochastic nature of mooring system failures, Latin Hypercube Sampling (LHS) was adopted to produce an additional 100 stiffness combination samples with unseen failures for machine learning testing and performance validation.<sup>25</sup>

# 3.2 Data-driven identification of mooring system damage

Following the database produced in Section 3.1.2, the data-driven model, i.e., a CNN model is established for efficient mooring system damage identification.

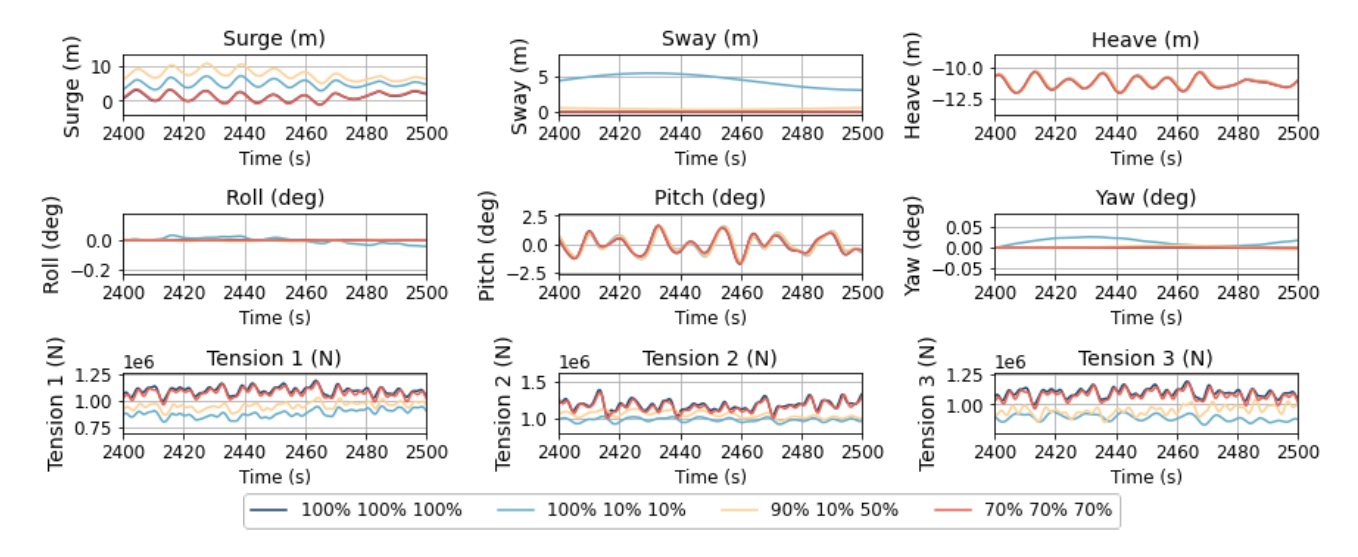


Figure 5. Dynamic responses of the floating platform for different stiffness combinations.

## 3.2.1 CNN model establishment

The dynamic responses of the FE model and the corresponding mooring line stiffness reductions are treated as the input and output of the CNN model, respectively. To evaluate the performance of the CNN model, common regression evaluation metrics, such as mean square error (MSE), mean absolute error (MAE), and coefficient of determination  $(R^2)$  are employed.  $R^2$  falls into the range [0,1]. The larger the  $R^2$  value, the better the accuracy. Their mathematical expressions are given as follows,

$$MSE = \frac{1}{n} \sum_{i=1}^{n} (y_i - \hat{y}_i)^2 , \qquad (11a)$$

$$MAE = \frac{1}{n} \sum_{i=1}^{n} |y_i - \hat{y}_i| , \qquad (11b)$$

$$R^{2} = 1 - \frac{\sum_{i=1}^{n} (y_{i} - \hat{y}_{i})^{2}}{\sum_{i=1}^{n} (y_{i} - \bar{y})^{2}},$$
(11c)

where  $y_i$  and  $\hat{y}_i$  represent the actual and predicted values, respectively.  $\bar{y}$  is the mean of the actual values  $y_i$ . n denotes the total number of data points. The CNN architecture and relevant hyperparameters are subject to tuning to ensure the adequate training of the model without underfitting or overfitting. In this research, the optimal CNN architecture is finalized with detailed configurations given in Table 2. Other key hyperparameters are set as follows: Learning rate: 0.01; Batch size: 32; Epoch size: 600; Optimizer: Adam.

#### 3.2.2 Result discussion

In the training stage, 800 of the 1,000 training data and the rest are used for model training and validation, respectively. The training history is shown in Fig. 6. As can be seen clearly, both the training and validation losses decrease with respect to epoch, and the training loss is slightly smaller than the validation loss when the training process approaches the end. Such observation demonstrates normal training without overfitting. Once the model is established, it is utilized to predict the stiffness reductions of mooring lines over 100 LHS samples, with the prediction accuracy using  $R^2$  given in Fig. 7. Clearly, the actual stiffness reductions agree well with predicted stiffness reductions, yielding  $R^2$  values that are all close to 1. This excellent testing accuracy serves as strong validation for the effectiveness of the proposed methodology.

To further verify the robustness of the CNN model, the K-fold cross-validation analysis is conducted. Specifically, we involve 1,000 training data and split them into 5 subsets for the 5-fold cross-validation analysis. The

Table 2. CNN model architecture adopted

Layer	Type	Input Size	Output Size	Trainable parameters <sup>1</sup>
Input Layer	-	(9, 18001)	(9, 18001)	
First Convolution	Conv1d	(9, 18001)	(64, 17999)	$(3 \times 9 + 1) \times 64 = 1792$
First Pooling	MaxPool1d	(64, 17999)	(64, 8999)	
Second Convolution	Conv1d	(64, 8999)	(128, 8997)	$(3 \times 64 + 1) \times 128 = 24704$
Second Pooling	MaxPool1d	(128, 8997)	(128, 4498)	
Flatten Layer	Flatten	(128, 4498)	$128 \times 498$	$(128 \times 4498 + 1) \times 3 = 1727235$
Fully Connected	Linear	$128 \times 4498$	3	,

<sup>&</sup>lt;sup>1</sup> Note: the total number of trainable parameters: 1,753,731.

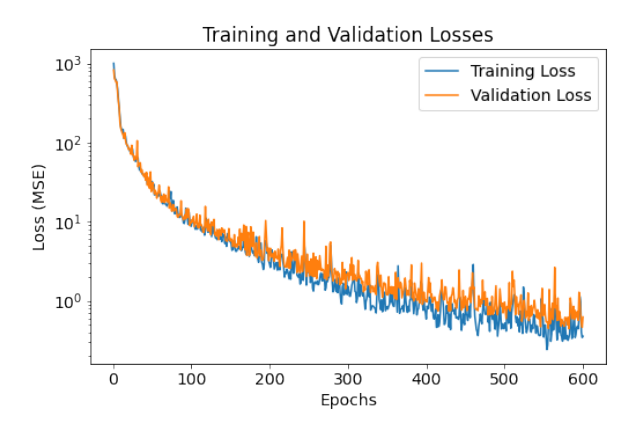


Figure 6. CNN model training history.

model is iterated 5 times to collect the validation results using different metrics, as shown in Fig. 8 and Table 3. From the above results, it can be found that the model shows a high degree of accuracy and performance robustness in damage identification of the mooring system. The accuracy for predicting the damage of the mooring line 2 is especially high. This may be attributed to the assumption that loads propagate mainly along the x-direction, <sup>24</sup> with mooring line 2 playing the role of the primary restoring force provider along this direction. It is also worth noting that no preprocessing effort is made for feature extraction, implying that the model can successfully identify the damage of the mooring system without complex feature engineering analysis. In summary, the proposed methodology has been demonstrated to be effective in identifying mooring system damage, which is critical for early detection and maintenance of the offshore infrastructure.

Table 3. CNN model architecture adopted

Fold	Mean Square		Mean Absolute		Coefficient of				
	Error $(MSE)$		Error $(MAE)$		Determination $(R^2)$				
1	0.6284	0.1416	0.2179	0.6666	0.2563	0.3332	0.9992	0.9998	0.9998
2	1.0910	0.3811	0.9078	0.8066	0.5300	0.6390	0.9987	0.9996	0.9989
3	0.7272	0.2535	0.5218	0.6627	0.4207	0.574	0.9991	0.9997	0.9993
4	0.1152	0.6983	0.4631	0.2341	0.4903	0.5081	0.9999	0.9991	0.9994
5	0.3775	0.1634	0.2652	0.4367	0.2820	0.3419	0.9995	0.9998	0.9997
Overall		0.4635			0.4788			0.9994	

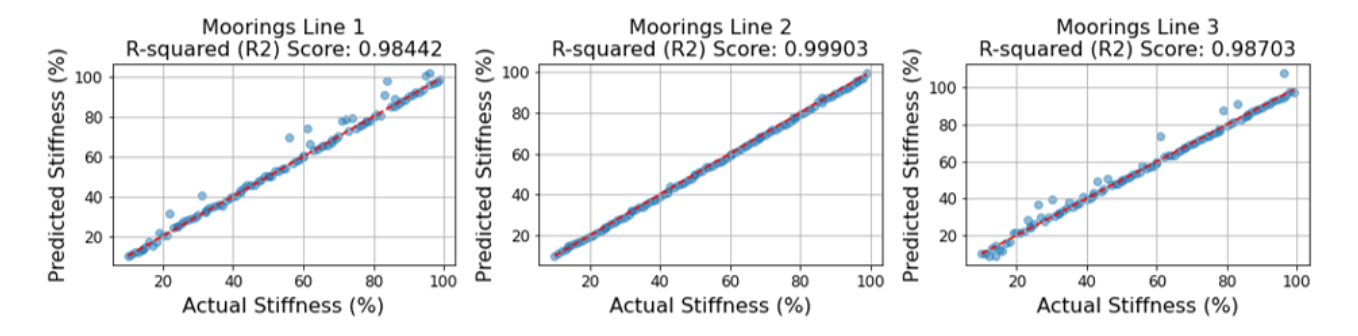


Figure 7. Testing result.

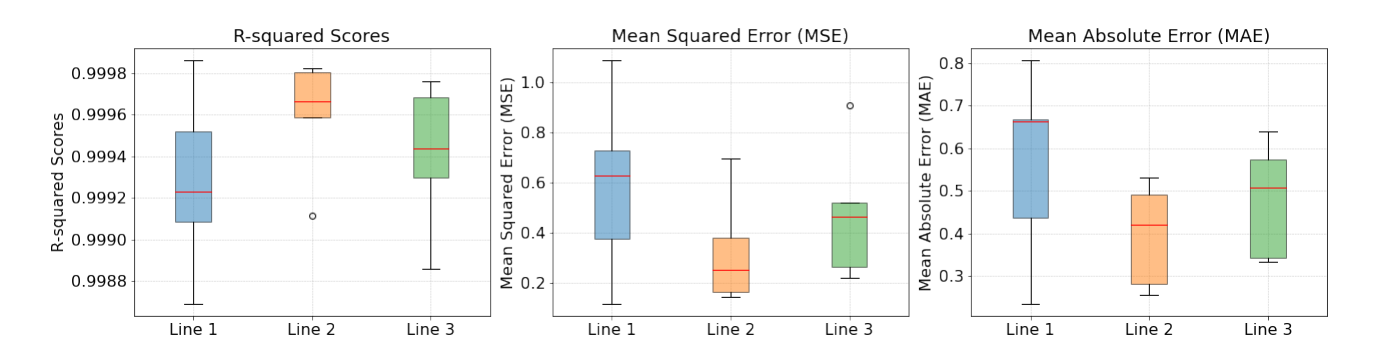


Figure 8. The cross-validation analysis results.

# 4. CONCLUSION AND FUTURE STUDY

In this study, an integrated framework that seamlessly integrates physical modeling with data-driven models to effectively identify damage in mooring systems of marine floating structures is developed. The fluid-structure interaction (FSI) finite element model is constructed as the mainstay of the framework, which guides the convolutional neural network (CNN) modeling and prediction. The proposed methodology has been practiced and the results demonstrate excellent damage prediction accuracy and robustness, offering strong support for future applications in marine infrastructure health management and maintenance. The future endeavor involves the incorporation of experimental measurement for further framework validation. In particular, remotely operated underwater vehicles (ROVs) equipped with cameras will be applied to conduct vision-based full-field measurements. The stochastic nature of the wave condition will be also considered in the damage identification task, necessitating the uncertainty analysis during the task. <sup>26,27</sup> Additionally, advanced methods will be developed to handle potential uncertainties, thereby further promoting the damage identification capacity.

## ACKNOWLEDGMENTS

This research is supported in part by NSF under grant CMMI - 2138522, and in part by start-up fund offered by The Hong Kong Polytechnic University.

#### REFERENCES

- [1] Moan, T., "Life cycle structural integrity management of offshore structures," Structure and Infrastructure Engineering 14(7), 911–927 (2018).
- [2] D'Souza, R. and Majhi, S., "Application of lessons learned from field experience to design, installation and maintenance of fps moorings," in [Offshore Technology Conference], OTC-24181, OTC (2013).
- [3] Nordgård-Hansen, E. M. and Schlanbusch, R., "Condition monitoring and maintenance for fibre rope moorings in offshore wind," (2023).
- [4] Zhou, K. and Tang, J., "Structural model updating using adaptive multi-response gaussian process metamodeling," *Mechanical Systems and Signal Processing* **147**, 107121 (2021).
- [5] Hua, X., Ni, Y., and Ko, J., "Adaptive regularization parameter optimization in output-error-based finite element model updating," *Mechanical Systems and Signal Processing* **23**(3), 563–579 (2009).
- [6] Zhou, K. and Tang, J., "Highly efficient probabilistic finite element model updating using intelligent inference with incomplete modal information," *Journal of Vibration and Acoustics* **138**(5), 051016 (2016).
- [7] Bae, Y., Kim, M., and Kim, H., "Performance changes of a floating offshore wind turbine with broken mooring line," Renewable Energy 101, 364–375 (2017).
- [8] Yang, Y., Bashir, M., Li, C., and Wang, J., "Investigation on mooring breakage effects of a 5 mw barge-type floating offshore wind turbine using f2a," *Ocean Engineering* **233**, 108887 (2021).
- [9] Tarantola, A., [Inverse problem theory and methods for model parameter estimation], SIAM (2005).
- [10] Amezquita-Sanchez, J. P. and Adeli, H., "Signal processing techniques for vibration-based health monitoring of smart structures," Archives of Computational Methods in Engineering 23, 1–15 (2016).
- [11] Alzubaidi, L., Zhang, J., Humaidi, A. J., Al-Dujaili, A., Duan, Y., Al-Shamma, O., Santamaría, J., Fadhel, M. A., Al-Amidie, M., and Farhan, L., "Review of deep learning: Concepts, cnn architectures, challenges, applications, future directions," *Journal of big Data* 8, 1–74 (2021).
- [12] LeCun, Y., Bengio, Y., and Hinton, G., "Deep learning," nature **521**(7553), 436–444 (2015).
- [13] Gu, J., Wang, Z., Kuen, J., Ma, L., Shahroudy, A., Shuai, B., Liu, T., Wang, X., Wang, G., Cai, J., et al., "Recent advances in convolutional neural networks," *Pattern recognition* 77, 354–377 (2018).
- [14] Gomez-Cabrera, A. and Escamilla-Ambrosio, P. J., "Review of machine-learning techniques applied to structural health monitoring systems for building and bridge structures," *Applied Sciences* **12**(21), 10754 (2022).
- [15] De Oliveira, M. A., Monteiro, A. V., and Vieira Filho, J., "A new structural health monitoring strategy based on pzt sensors and convolutional neural network," Sensors 18(9), 2955 (2018).
- [16] ANSYS, Inc., ANSYS Aqwa Theory Manual. ANSYS, Inc., 275 Technology Drive, Canonsburg, PA 15317, USA, 15.0 ed. (Nov. 2013). Certified to ISO 9001:2008.
- [17] Ghafari, H. and Dardel, M., "Parametric study of catenary mooring system on the dynamic response of the semi-submersible platform," *Ocean Engineering* **153**, 319–332 (2018).
- [18] Mao, Y., Zheng, M., Wang, T., and Duan, M., "A new mooring failure detection approach based on hybrid lstm-svm model for semi-submersible platform," *Ocean Engineering* **275**, 114161 (2023).
- [19] Cummins, W. et al., "The impulse response function and ship motions," (1962).
- [20] Bao, X., Fan, T., Shi, C., and Yang, G., "One-dimensional convolutional neural network for damage detection of jacket-type offshore platforms," *Ocean Engineering* **219**, 108293 (2021).
- [21] Kiranyaz, S., Avci, O., Abdeljaber, O., Ince, T., Gabbouj, M., and Inman, D. J., "1d convolutional neural networks and applications: A survey," *Mechanical systems and signal processing* **151**, 107398 (2021).
- [22] Liu, Z., Tianhui, F., and Chaonuclear, C., "Comparative hydrodynamic performance analysis of three typical semi-submersible floating wind turbine foundations," *China Offshore Platform* **36**(2), 1–10 (2021).
- [23] Huang, X., Liu, Y., Liu, J., et al., "Mooring cable layout and fracture simulation analysis of deepcwind platform of offshore wind turbine," *Science Technology and Engineering* **23**(6), 2419–2427 (2023).
- [24] Robertson, A., Jonkman, J., Masciola, M., Song, H., Goupee, A., Coulling, A., and Luan, C., "Definition of the semisubmersible floating system for phase ii of oc4," Tech. Rep. NREL/TP-5000-60601, National Renewable Energy Lab. (NREL), Golden, CO (United States) (2014).

- [25] Minasny, B. and McBratney, A. B., "A conditioned latin hypercube method for sampling in the presence of ancillary information," *Computers & geosciences* **32**(9), 1378–1388 (2006).
- [26] Zhou, K. and Tang, J., "Uncertainty quantification of mode shape variation utilizing multi-level multi-response gaussian process," *Journal of Vibration and Acoustics* **143**(1), 011003 (2021).
- [27] Zhou, K. and Tang, J., "Efficient characterization of dynamic response variation using multi-fidelity data fusion through composite neural network," *Engineering Structures* **232**(1), 111878 (2021).